Magnetic properties of nearly defect-free maghemite nanocrystals

P. Dutta, A. Manivannan, and M. S. Seehra*
Physics Department, West Virginia University, Morgantown, West Virginia 26506-6315, USA

N. Shah and G. P. Huffman
Consortium for Fossil Fuel Science, University of Kentucky, Lexington, Kentucky 40506, USA
(Received 19 April 2004; revised manuscript received 10 August 2004; published 17 November 2004)

Temperature variations of the magnetization M and the electron magnetic resonance (EMR) parameters of maghemite (γ-Fe_2O_3) nanocrystals are reported for the 4 K–300 K range. Transmission electron microscopy of the nanocrystals shows them to be nearly spherical samples (aspect ratio $a/b=1.15$) with diameter $D=7(1)$ nm, and analysis of x-ray diffraction lines yields $D=6.4$ nm with negligible strain. M versus T data show blocking temperatures $T_B \simeq 101$ K, 89 K, and 68 K in measuring fields $H=50$, 100, and 200 Oe respectively. M versus H data for $T>T_B$ fits the modified Langevin function $M=M_s\mathcal{L}(\mu_p H/k_B T)+\chi_a H$ with $\mu_p=8000(500)\mu_B$/particle and $M_s=80$ emu/g, identical to M_s for bulk γ-Fe_2O_3. It is argued that this large value of M_s, the small value of coercivity $H_c \simeq 20$ Oe at 5 K, the lack of exchange bias in a field-cooled sample, and negligible strain point to nearly defect-free nanocrystals. In the EMR studies, two resonance lines are observed, one with the resonance field H_r greater than that for the free-electron value and the other smaller. From the temperature variations of H_r and the linewidths of the two lines, it is argued that the two lines are, respectively, due to nanocrystals with easy-axis aligned perpendicular and parallel to the applied field. The relatively narrow intrinsic linewidths ($\simeq$400 Oe) of the two lines in nearly defect-free nanocrystals facilitated their observation.

DOI: 10.1103/PhysRevB.70.174428 PACS number(s): 75.50.Tt, 76.40.+b, 75.50.Gg, 75.30.Cr

I. INTRODUCTION

Magnetite (Fe_3O_4) and maghemite (γ-Fe_2O_3) are two of the important oxides of iron with ferrimagnetic ordering and hence substantial magnetization M_s at room temperature. Consequently, these oxides, particularly in the nanoparticle (NP) size range, have found numerous applications such as in high-density magnetic storage,[1,2] as ferrofluids,[3,4] and in the biomedical area.[5] Recently, there have been a number of reports on the synthesis and magnetic properties of γ-Fe_2O_3 NP of different shapes and sizes.[6–12] However, a definite picture as to how magnetic properties change with change in particle size has not emerged from these studies. Measurements reported by Martinez *et al.*[6] on γ-Fe_2O_3 platelets of size 10 nm with diameter/thickness $\simeq$4 showed a blocking temperature $T_B \simeq 75$ K and a spin-glass freezing of surface layer spins at $T_F \simeq 42$ K. Surprisingly, M_s at 60 kOe in these particles was only about 5 emu/g, substantially smaller than $M_s \simeq 80$ emu/g for bulk γ-Fe_2O_3. Also large magnitudes of exchange bias H_e and coercivity $H_c \simeq 2$ kOe were observed at 5 K. In the magnetization/electron magnetic resonance (EMR) studies of Koksharov *et al.*[7,8] on 2.5 nm NP imbedded in polyethylene matrix, a single EMR line along with $T_B \simeq 75$ K and $T_F \simeq 40$ K were reported. Magnetic studies by Dormann *et al.*[11] showed how T_B and the field-cooled (FC) magnetic susceptibility (χ) are affected by interparticle interactions. The EMR studies by Netzelmann[8] on magnetic recording tapes of γ-Fe_2O_3 showed the shifts of the resonance lines due to a demagnetization field so that EMR lines even for applied field H within the plane of the tape occur at different fields because of the differences in the length and width of the film.

The Mössbauer spectroscopy studies of Serna *et al.*[12] on two different γ-Fe_2O_3 NP of about the same size (3.5 nm) but prepared using slightly different methods showed that the large differences in the measured internal fields and the coercivity H_c between the two samples must be due to structural disorder. They suggested that this structural disorder occurs not only at the surface layer but also in the interior of the particles. Since γ-Fe_2O_3 has inherent cation vacancies V in the octahedral positions according to the formula $4Fe_2O_3 \rightarrow 3\{Fe^{3+}O\cdot(Fe^{3+}_{5/3}V_{1/3})O_3\}$, the different degree of order-disorder at different sites might be affected by the preparation method.

In this work, we report magnetization and EMR studies in nearly spherical particles of γ-Fe_2O_3 of 7 nm diameter. What distinguishes our results from earlier studies is that the measured $M_s \simeq 80$ emu/g in these nanoparticles is equal to the bulk value, with negligible coercivity and no exchange bias below $T_B \simeq 100$ K. This suggests that these nanoparticles are near perfect crystals without significant disorder. In EMR studies, two resonance lines are observed which are interpreted in terms of particles with easy axis aligned parallel and perpendicular to the applied field. For $T>T_B$, the M versus H fits the Langevin variation with magnetic moment/particle $\mu_p \simeq 8000\ \mu_B$. Details of the synthesis, characterization, and magnetic properties of these nanoparticles are given below.

II. SYNTHESIS

Synthesis of the γ-Fe_2O_3 nanoparticles of controlled size was carried out using a slightly modified route of well established thermolysis procedure.[13–16] Mixture of 2.57 gm oleic acid and 20 mL of octyl ether was heated to about 100 °C. 0.4 mL of $Fe(CO)_5$ was added to the mixture. This mixture was refluxed (at about 280 °C) for 1 h. After cooling the

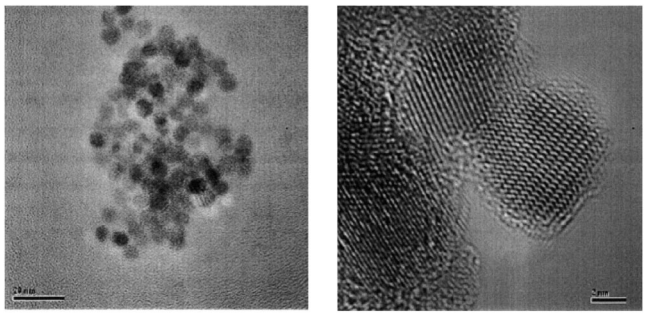

FIG. 1. TEM micrographs of the γ-Fe_2O_3 nanocrystals at two different magnifications. The bar length on the left (right) picture is 20 nm (2 nm).

mixture to room temperature, 0.68 g of $(CH_3)_3NO$ was added to it. The solution was reheated to about ~130 °C for 2 h and refluxed for an additional hour. Ethanol was added to the cooled mixture and the nanoparticles were centrifuged to the bottom. A small quantity of Fe-oxide nanoparticles suspended in ethanol was diluted in acetone and sonicated. A drop of this acetone solution was placed on a transmission electron microscopy (TEM) grid for TEM analysis. A dry powder of nanoparticles was obtained by simply letting the ethanol evaporate for further characterization.

III. STRUCTURAL CHARACTERIZATION

The TEM studies (Fig. 1) show the particles to be ellipsoidal with major/minor axis ratio $\simeq$1.15 and average size $\simeq$7(1) nm. The room-temperature x-ray diffraction (XRD) pattern using Cu $K\alpha$ radiation ($\lambda = 0.154\,185$ nm) is shown in Fig. 2 along with similar data on a bulk γ-Fe_2O_3 sample obtained from Alfa-Aesar. The width β of the peaks (after correction for instrumental broadening) was used to determine the average grain size D and the strain η using the relation[17]

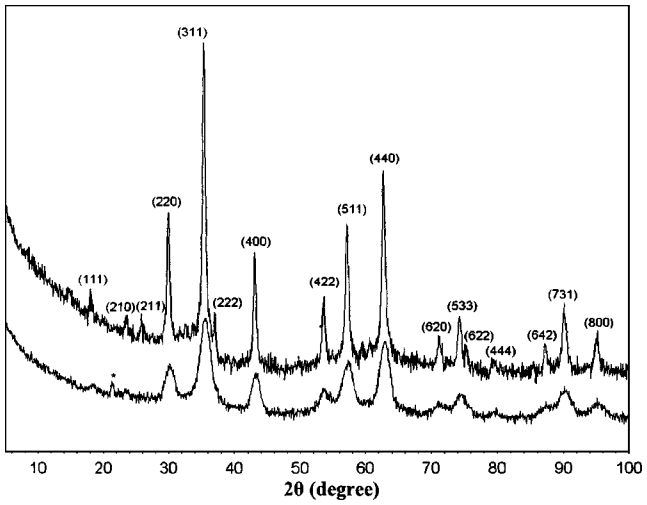

FIG. 2. Room-temperature x-ray diffraction patterns of the γ-Fe_2O_3 nanoparticles (bottom) and a commercial bulk γ-Fe_2O_3 (top). The miller indices of the lines are noted. The line marked with an asterisk is identified with silica impurity.

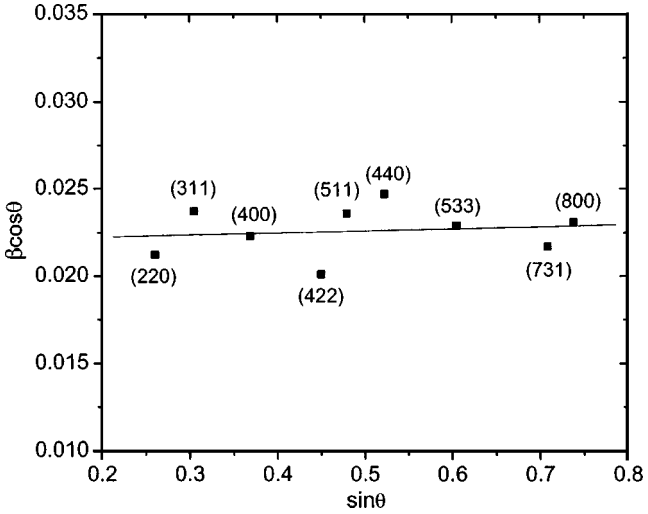

FIG. 3. Plot of $\beta\cos\theta$ vs $\sin\theta$ using several lines of γ-Fe_2O_3 NP. The solid line is a least-squares fit to Eq. (1) yielding $D = 6.4$ nm and $\eta = 1.2\times10^{-3}$.

$$\beta\cos\theta = \frac{0.89\lambda}{D} + \eta\sin\theta. \tag{1}$$

The plot of $\beta\cos\theta$ versus $\sin\theta$ using different Bragg lines of Fig. 2 yields $D \simeq 6.4$ nm and a negligible $\eta \simeq 1.2\times10^{-3}$ (Fig. 3). This analysis shows that the NPs of γ-Fe_2O_3 are essentially strain-free with size similar to that determined by TEM.

IV. EXPERIMENTAL RESULTS AND DISCUSSION

A. Magnetization

The temperature (T) and magnetic field (H) variations of the magnetization M were measured with a commercial SQUID (superconducting quantum interference device) magnetometer. The temperature variations of M for the zero-field-cooled (ZFC) and the field-cooled (FC) cases measured in $H = 50$, 100, and 200 Oe are shown in Fig. 4. The blocking temperature T_B at which the ZFC magnetization peaks decreases as H is increased, as expected for a superparamagnet.[18] However, unlike some earlier reports,[6,7] there is no indication of an anomalous change in χ(FC) below T_B, characteristic of a surface spin-glass transition near 40 K. Spin-glass ordering of the surface spins below T_B was also reported recently in ferrihydrite nanoparticles.[19]

The variations of M versus H at $T = 300$, 250, 200, and 5 K are shown in Fig. 5. Since M versus H has a nonzero slope even at higher H, we have fitted this variation to the modified Langevin function,[19–21]

$$M = M_s\mathcal{L}(\mu_p H/k_B T) + \chi_a H, \tag{2}$$

where μ_p is the magnetic moment/particle, k_B is the Boltzmann constant, $\mathcal{L}(x) = \coth x - 1/x$, and χ_a is the high-field susceptibility. The plot of $(M - \chi_a H)/M_s$ versus H/T for $T = 300$, 250, and 200 K shown in Fig. 6 collapses onto a single curve, signifying superparamagnetism with $\mu_p \simeq 8000(500)\mu_B$, whereas a similar analysis for the data at

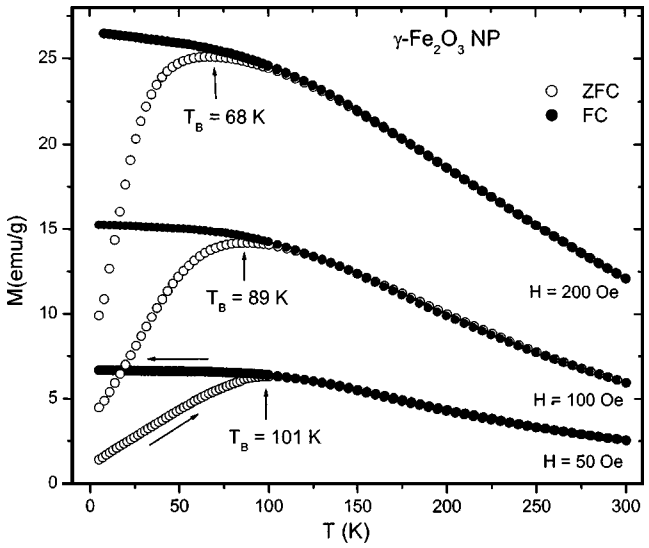

FIG. 4. Temperature dependence of the magnetization M for γ-Fe_2O_3 NP in applied fields $H=50$, 100, and 200 Oe under the FC (field-cooled) and ZFC (zero-field-cooled) conditions. Arrows indicate the direction of temperature changes, with T_B defined by the peak value of the ZFC curve (vertical arrows).

5 K shows a large departure from this fit as expected for $T<T_B$. The magnitudes of μ_p can also be determined from the equation $\mu_p=M_s\rho V$, where ρ and V are, respectively, the density and volume of the particle. Assuming a spherical particle with diameter $D=7$ nm, $\rho=4.86$ g/cm^3 for γ-Fe_2O_3 and $M_s=80(85)$emu/g, yields $\mu_p\simeq 7500(8000)\mu_B$, in agreement with the above estimate determined from the fit to Eq. (2).

The M versus T data of Fig. 4 are measured at relatively small $H=50$, 100, and 200 Oe for which the approximation $\mu_pH/k_BT<1$ is valid for $T>T_B$ even for $\mu_p\simeq 8000\ \mu_B$. For example, for $H=50$ Oe and $T=200$ K, $\mu_pH/k_BT=0.134$. Therefore, in the expansion of $\mathcal{L}(x)=(x/3)-(x^3/45)+\cdots$, the approximation $\mathcal{L}(x)=x/3$ is valid. Using this in Eq. (2) yields

$$\chi=\partial M/\partial H=\chi_a+(M_s\mu_p/3k_BT) \tag{3}$$

which is just a special case of Eq. (2) for $\mu_pH/k_BT\ll 1$. Since both χ_a and M_s are temperature-dependent (see the inset of Fig. 6), the simple Curie-law variation of $\chi\sim 1/T$ is not strictly valid, as discussed in detail in a recent paper on antiferromagnetic nanoparticles.[22] Consequently, the magnitude of μ_p from Eq. (3) can be determined only if some functional forms of the temperature dependence of M_s and χ_a are assumed.[22] Nevertheless, χ(FC) for a noninteracting superparamagnet is expected to continue to increase with decrease in temperature approximately as $1/T$.[20] The deviations from this variation of χ(FC) observed in Fig. 4 for $T<T_B$ are due to interparticle interactions.[23–26] Further discussion on the interparticle interactions is given later in the paper. The sources of χ_a in Eq. (2) include any deviations from ideal magnetic order such as disorder and canting of the sublattices under an applied field. This issue is discussed in some detail in Ref. 20.

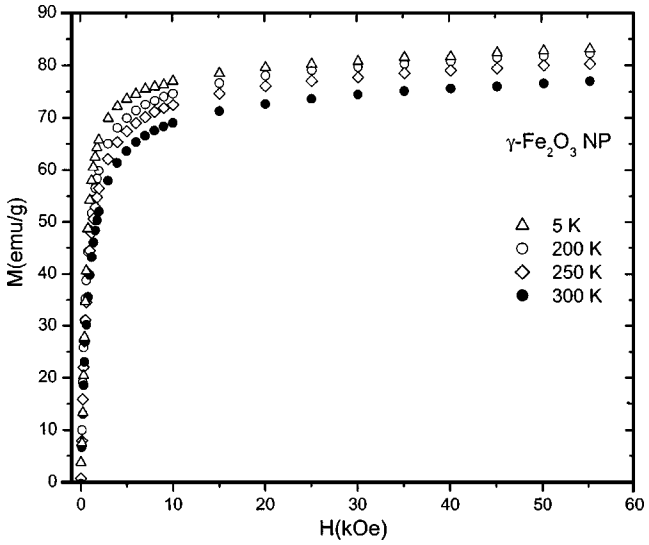

FIG. 5. Magnetization M measured as a function of applied field H at temperatures indicated.

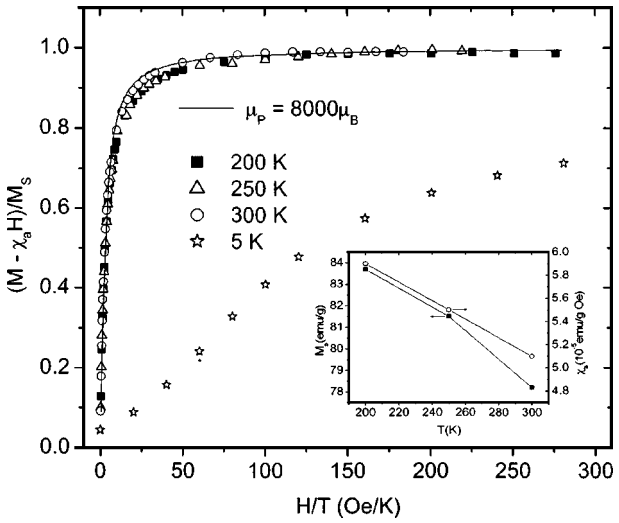

FIG. 6. Plot of $(M-\chi_aH)/M_s$ vs H/T using the data at $T=5$, 200, 250, and 350 K. The solid line is fit to Eq. (2) with $\mu_p=8000\ \mu_B$. The data at 5 K depart from the fit as expected for $T<T_B$. The inset shows temperature variations of M_s and χ_a determined from the fit.

The hysteresis loops measured at 5 K, both for the ZFC case and the case where the sample was cooled from 300 K to 5 K in 20 kOe, are shown in Fig. 7. The coercivity H_c is only around 20 Oe, with no measurable loop shift H_e for the FC case. This is in great contrast to the magnitudes of around 2 kOe for H_c and H_e reported by Martinez *et al.* in γ-Fe_2O_3 NP (Ref. 6) and $H_c\simeq 1$ kOe reported by Vassiliou *et al.* in 8.5 nm nanocrystals of γ-Fe_2O_3.[27] We attribute these differences to the considerable amount of structural disorder present in their sample, following the arguments of Serna *et al.*[12] Using $H_c\simeq K/2M_s\rho$ yields the anisotropy energy $K=1.65\times 10^4$ erg/cm^3 for $M_s=80$ emu/g and $H_c=20$ Oe. This relatively small magnitude of K is expected since Fe^{3+} ions in γ-Fe_2O_3 have angular

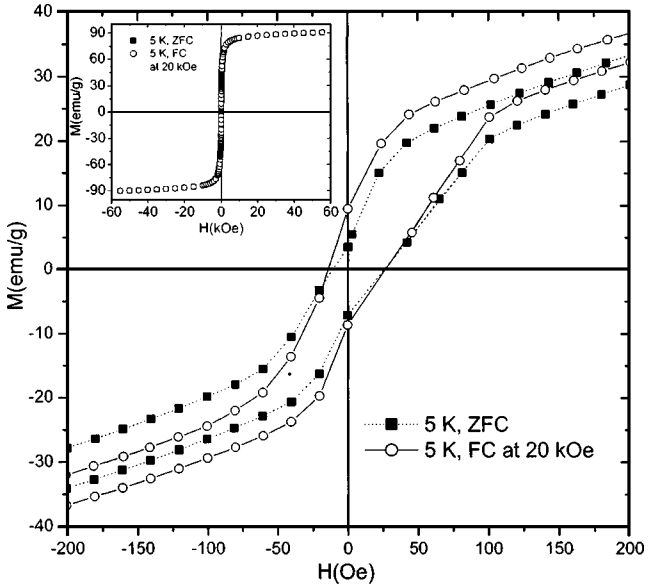

FIG. 7. Hysteresis loop of γ-Fe_2O_3 NP measured at 5 K under ZFC and FC at 20 kOe. The inset shows the full loop to ±55 kOe.

momentum $L=0$ in their ground state. This value of K is an order of magnitude smaller than reported previously[28] in nm size particles of γ-Fe_2O_3. Again, atomic disorder will increase H_c and hence K so that K may differ substantially for samples with different degrees of disorder.

B. Electron magnetic resonance (EMR) experiments

The EMR experiments were carried out at 9.28 GHz using a standard reflection type spectrometer and an Oxford Instruments cryostat for variable temperature studies from 4 K to 300 K. Two resonance lines are observed whose resonance field H_r and the peak-to-peak linewidth ΔH were measured as a function of temperature. For comparison, same parameters were measured for the single line observed in the bulk sample of γ-Fe_2O_3 whose XRD pattern is shown in Fig. 2.

The observed EMR spectra (absorption derivative) of the samples are shown in Figs. 8(a) and 8(b) at the temperatures shown, whereas the temperature variations of H_r for the two lines (low-field line A and high-field line B) of γ-Fe_2O_3 NP and the single line of bulk γ-Fe_2O_3 are shown in Fig. 9. Similarly, the temperature variations of ΔH for these lines are shown in Fig. 10. It is noted that H_r for the single line of bulk γ-Fe_2O_3 is about the average of the two lines observed in the γ-Fe_2O_3 NP, whereas ΔH for the bulk line is several times the individuals ΔH for the two lines of γ-Fe_2O_3 NP. This may explain why in the earlier reported studies of γ-Fe_2O_3, only a single broad line has been reported, presumably because of excessive structural defects in these samples. For cubic γ-Fe_2O_3 with negative anisotropy constant K, the numerical calculations of Valstyn *et al.*[28] predicted four different resonance frequencies for nearly spherical samples and two resonance frequencies for ellipsoidal samples with $a/b \geqslant 1.30$. However, only a single resonance mode was observed in their bulk samples. The two-line pattern reported here in γ-Fe_2O_3 is perhaps a confirmation of this prediction, as discussed in more detail later.

The temperature dependence of H_r for the low-field line A (Fig. 9) is very similar to that reported in other NP systems[21,29–32] and in γ-Fe_2O_3 reported by others[7,8] in that H_r decreases as T decreases. On the other hand, for the high-field line B, H_r is essentially independent of temperature, with only a minor decrease below $T_B \simeq 100$ K (Fig. 9). The

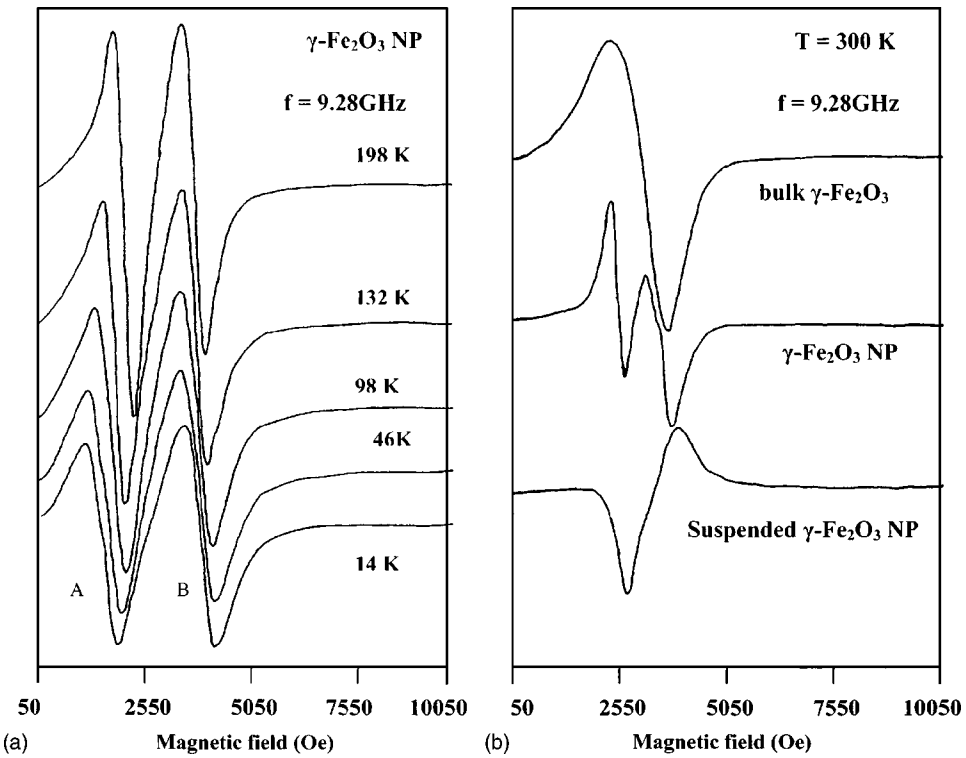

FIG. 8. Absorption derivative EMR spectra of (a) γ-Fe_2O_3 NP at several temperatures and (b) bulk γ-Fe_2O_3, γ-Fe_2O_3 NP, and γ-Fe_2O_3 NP suspension in ethanol at room temperature. The magnetic field scan starts from 50 Oe (rather than zero), because for $H<50$ Oe the field of the electromagnet is not stable.

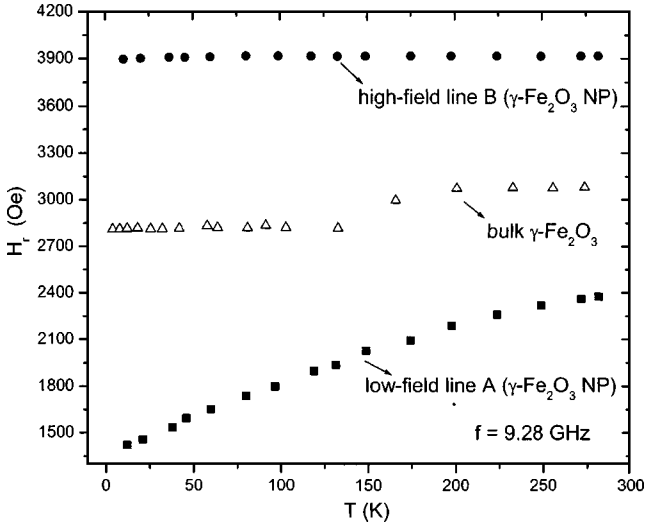

FIG. 9. Temperature variations of the resonance field H_r for the two EMR lines of γ-Fe_2O_3 NP and for the single line of bulk γ-Fe_2O_3.

behavior of ΔH versus T shown in Fig. 10 for lines A and B shows that for $T<T_B$, ΔH are nearly equal for the two lines, although continuing to increase with decrease in T as also observed in other NP systems.[7,21,29–32] The line intensity $(\Delta H)^2\ell$ (ℓ is the peak-to-peak height of the absorption derivative) for the two lines also become equal for $T<T_B$ (Fig. 11). The increase in the line intensity with a decrease in temperature qualitatively follows the temperature variation of the magnetization, Eq. (2), as expected.

According to the model of Nagata and Ishihara,[29] the shift in the resonance field δH_r and the linewidth ΔH are due to demagnetizing fields of nonspherical samples and they are related by $\delta H_r \sim (\Delta H)^n$, where $n=2$ for partially oriented and $n=3$ for randomly oriented NP systems. This relation has been verified in a number of systems.[7,21,29,30] For the low-field line A, the plot of ln δH_r versus ln ΔH is shown in Fig.

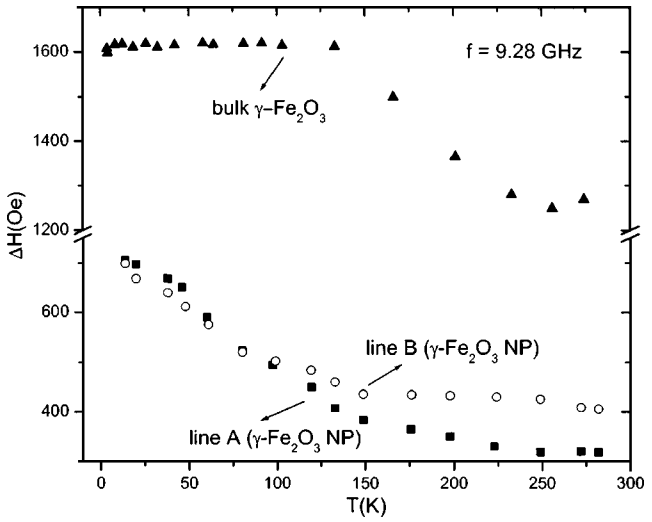

FIG. 10. Temperature variations of the linewidth ΔH of the two EMR lines (line A and line B) of γ-Fe_2O_3 NP and that of the single line of bulk γ-Fe_2O_3.

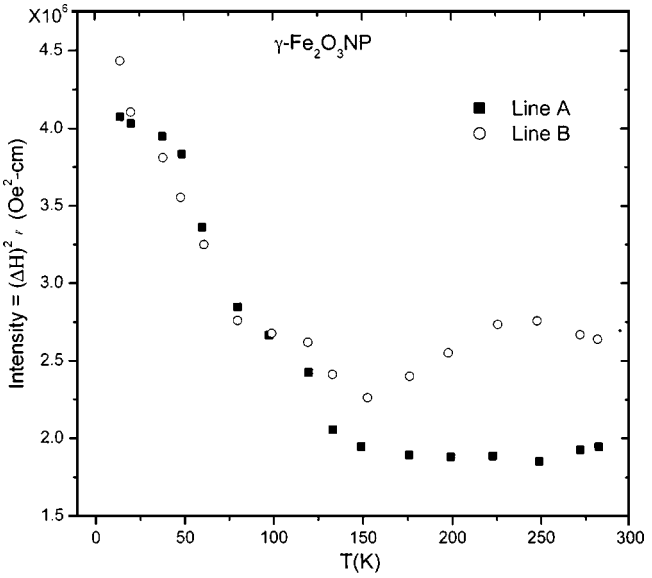

FIG. 11. Temperature variation of the line intensity $=(\Delta H)^2\ell$ for the two EMR lines of the γ-Fe_2O_3 NP.

12, where $\delta H_r = 3315 - H_r$ corresponding to $g=2$ and $f=9.28$ GHz has been used. The slope $n=1.5$ for $T>130$ K and $n=0.75$ for $T<130$ K. These lower values of n are consistent with a partially ordered system.

To understand the origin of the high-field line B, we refer to the theory of Raikher and Stepanov[33] on the effect of thermal fluctuation and anisotropy on the EMR in single domain NP of dispersed ferromagnets for the case of intrinsic anisotropy field $H_a \ll H_r$. For $T>T_B$, the effect of temperature is to induce a random fluctuating field $H_f \sim k_B T/\mu_p$, thereby narrowing the line with an increase in temperature. The grains for which the applied field is parallel to the easy axis have a lower H_r than that for grains with easy axis perpendicular to the applied field, thus giving a two-line pattern. The numerical simulation for $H_a/H \simeq 0.1$ and low T

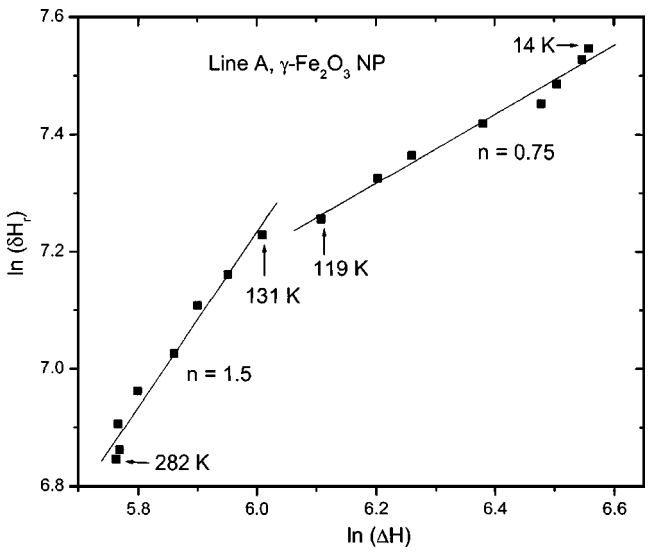

FIG. 12. Plot of ln ΔH_r vs ln ΔH for the low-field line A of γ-Fe_2O_3 NP. Change in the slope n occurs near $T_B \simeq 100$ K.

yielded $H_r \simeq 3650$ Oe for the high-field line and $H_r \simeq 2650$ Oe for the low-field line.[33] These estimates are close to our experimental observations in Fig. 9. Another important prediction of the Raihker-Stepanov model[33] is that the difference between H_r of the two lines decreases with an increase in T, as also observed in Fig. 9, so that at high enough temperature, only a single line should be observed. This temperature is not achieved in our experiments, which are limited to room temperature and below.

It is well known that in a solid with anisotropic g factor g_1, g_2, and g_3, the EMR spectra of its powder will have three lines at $H_r = hf/g_i\mu_B$ (h is Planck's constant) if ΔH of individual components is smaller than the separation between the lines.[34] As ΔH becomes larger, the components at the lowest and highest fields become obscured. Also, if the anisotropic solid rotates randomly with correlation time $\ll h/2\pi(g_1 - g_3)\mu_B H$, then a single line is obtained at the average $g_0 = (g_1+g_2+g_3)/3$. To check this latter scenario, we suspended our γ-Fe_2O_3 NP in ethanol and took their EMR spectra at room temperature. The spectra of this suspension, also shown in Fig. 8(b), gives a broad line with $\Delta H \simeq 1270$ Oe and $H_r \simeq 3290$ Oe, corresponding to $g \simeq 2$. It is suggested that this observed line shape is a superposition of two lines, due to random Brownian motion of the nanoparticles in the suspension.

V. CONCLUDING REMARKS

The conclusion drawn from the above discussion is that the two-line pattern observed in our γ-Fe_2O_3 NP is due to uniaxial anisotropy of the demagnetizing fields produced by nonspherical shapes of the particles. The low-field line A (high-field line B) is due to particles with major axis aligned parallel (perpendicular) to the applied field. The reason we have observed these two lines whereas earlier reports failed to do so is because of the narrow lines of our samples, presumably because our samples are nearly free from structural defects. The evidence for this is high values of M_s in our samples, essentially equal to M_s reported for bulk samples.[28] For the commercial bulk sample used here, we measured $M_s = 58$ emu/g and $H_c \simeq 70$ Oe at room temperature, indicating that this sample has also a significant degree of structural defects. Consequently, this work has demonstrated a close relationship between the observed magnetic properties of γ-Fe_2O_3 NP and the structural disorder. In this connection, a recent report[35] has shown that whereas γ-Fe_2O_3 has negligible H_c, ε-Fe_2O_3 with orthorhombic structure has $H_c \simeq 20$ kOe at room temperature.

For superparamagnetic noninteracting nanoparticles, the blocking temperature T_B determined by dc magnetization measurements is related to the anisotropy K and volume V of NP by the relation $T_B \simeq KV/30k_B$ (see, e.g., Refs. 19 and 20). Using $T_B \simeq 100$ K for $D = 7$ nm particles in our case yields $K = 2.3 \times 10^6$ erg/cm^3 and the corresponding anisotropy field $H_a \simeq K/2M_s\rho \simeq 2.8$ kOe. This magnitude of K (and hence H_a) is nearly an order of magnitude higher than the estimates for intrinsic K. However, it is well established that interparticle dipole-dipole interaction lowers the measured χ, lowers the Mossbauer T_B, but increases the T_B measured by magnetization studies.[11,23–26] For our compact powder of γ-Fe_2O_3, interparticle interactions are clearly present as indicated earlier following the discussion of Figs. 4 and 6. Hence the above relation for T_B is not valid. Using $a/b = 1.15$ for our ellipsoidal samples yields the demagnetization factors $D_a = 3.73$, $D_b = D_c = 4.42$, and demagnetization anisotropy field $H_D = (D_b - D_a)M_s\rho = 268$ Oe. For a sample with random orientation of particles, the Stoner-Wohlfarth[36] model which assumes coherent rotation of M under applied field yields $H_c \simeq H_D/2 = 134$ Oe. However, the measured $H_c \simeq 20$ Oe is even smaller than the above estimate. This lowered H_c is likely due to interparticle interactions since recent Monte Carlo simulation studies have shown that dipolar interactions lower H_c compared to corresponding values for noninteracting assembly of ferromagnetic nanoparticles.[37]

ACKNOWLEDGMENT

This research was supported by the U.S. Department of Energy, Contract No. DE-FC26-02NT41594, through the Consortium for Fossil Fuel Science.

*Corresponding author. Email address: mseehra@wvu.edu

[1] See the review by J. L. Dormann, D. Fiorani, and E. Tronc, on *Magnetic Relaxation in Fine-Particle Systems*, in *Advances in Chemical Physics, Vol. XCVIII*, edited by I. Prigogine and S. A. Rice (John Wiley, New York, 1997), pp. 283–494.

[2] D. E. Speliotis, J. Magn. Magn. Mater. **193**, 29 (1999), and references therein.

[3] F. L. Calderon, T. Stora, O. M. Monval, P. Poulin, and J. Bibette, Phys. Rev. Lett. **64**, 539 (1990).

[4] V. K. Sharma and F. Waldner, J. Appl. Phys. **48**, 4298 (1977).

[5] C. C. Berry and A. S. G. Curtis, J. Phys. D **36**, R198 (2003).

[6] B. Martinez, X. Obradors, Le. Balcells, A. Rouanet, and C. Monty, Phys. Rev. Lett. **80**, 181 (1998).

[7] Yu. A. Koksharov, S. P. Gubin, I. D. Kosobudsky, G. Yu. Yurkov, D. A. Pankratov, L. A. Ponomarenko, M. G. Mikheev, M. Beltran, Y. Khodorkovsky, and A. M. Tishin, Phys. Rev. B **63**, 012407 (2000).

[8] Yu. A. Koksharov, S. P. Gubin, I. D. Kosobudsky, M. Beltran, Y. Khodorkovsky, and A. M. Tishin, J. Appl. Phys. **88**, 1587 (2000).

[9] U. Netzelmann, J. Appl. Phys. **68**, 1800 (1990).

[10] S. Chakrabarti, S. K. Mandal, B. K. Nath, D. Das, D. Ganguli, and S. Chandhuri, Eur. Phys. J. B **34**, 163 (2003).

[11] P. Prené, E. Tronc, J. P. Jolivet, J. Livage, R. Cherkaoui, M. Nogués, J. L. Dormann, and D. Fiorani, IEEE Trans. Magn. **29**, 2658 (1993).

[12] C. J. Serna, F. Bodker, S. Morup, M. P. Morales, F. Sandiumenge, and S. Veintemillas-Verdauguer, Solid State Commun. **118**, 437 (2001).

[13] S. Sun, C. B. Murray, D. Weller, L. Folks, and A. Moser, Science **287**, 1989 (2000).

[14] T. Hyeon, S. S. Lee, J. Park, Y. Chung, and H. B Na, J. Am.

Chem. Soc. **123**, 12 798 (2001).
[15] C. Pathmamanoharan, N. L. Zuiverloon, and A. P. Philipse, Prog. Colloid Polym. Sci. **115**, 141 (2000).
[16] V. F. Puntes, K. M. Krishnan, and A. P. Alivisatos, Science **291**, 2115 (2001).
[17] M. M. Ibrahim, J. Zhao, and M. S. Seehra, J. Mater. Res. **7**, 1856 (1992); H. P. Klug and L. E. Alexander, *X-Ray Diffraction Procedures* (John Wiley, New York, 1974).
[18] J. L. Dormann, D. Fiorani, and M. E. Yamani, Phys. Lett. A **120**, 95 (1987); M. El-Hilo, K. O. Grady, and R. W. Chantrell, J. Magn. Magn. Mater. **114**, 307 (1992).
[19] A. Punnoose, T. Phanthavady, M. S. Seehra, N. Shah, and G. P. Huffman, Phys. Rev. B **69**, 054425 (2004).
[20] S. A. Makhlouf, F. T. Parker, and A. E. Berkowitz, Phys. Rev. B **55**, R14 717 (1997).
[21] M. S. Seehra, P. Dutta, H. Shim, and A. Manivannan, Solid State Commun. **129**, 721 (2004).
[22] M. S. Seehra and A. Punnoose, Phys. Rev. B **64**, 132410 (2001).
[23] R. W. Chantrell, N. Walmsley, J. Gore, and M. Maylin, Phys. Rev. B **64**, 024410 (2000).
[24] J. L. Dormann, L. Bessais, and D. Fiorani, J. Phys. C **21**, 2015 (1988).
[25] S. Morup, F. Bodker, P. V. Hendriksen, and S. Linderoth, Phys. Rev. B **52**, 287 (1995).
[26] S. Morup, Europhys. Lett. **28**, 671 (1994); S. Morup and E. Tronc, Phys. Rev. Lett. **72**, 3278 (1994).
[27] J. K. Vassiliou, V. Mehrotra, M. W. Russell, E. P. Giannelis, R. D. McMichael, R. D. Shull, and R. F. Ziolo, J. Appl. Phys. **73**, 5109 (1993).
[28] E. P. Valstyn, J. P. Hanton, and A. H. Morrish, Phys. Rev. **128**, 2078 (1962).
[29] K. Nagata and A. Ishihara, J. Magn. Magn. Mater. **104–107**, 1571 (1992).
[30] M. S. Seehra, A. Punnoose, P. Roy, and A. Manivannan, IEEE Trans. Magn. **37**, 2007 (2001).
[31] M. Ibrahim, G. Edwards, M. S. Seehra, B. Ganguly, and G. P. Huffman, J. Appl. Phys. **75**, 5873 (1994).
[32] F. Gazeau, J. C. Bacri, F. Gendron, R. Perzynski, Yu. L. Raikher, V. I. Stepanov, and E. Dubois, J. Magn. Magn. Mater. **186**, 175 (1998).
[33] Yu. L. Raikher and I. Stepanov, Sov. Phys. JETP **75**, 764 (1992); Phys. Rev. B **50**, 6250 (1994).
[34] C. P. Poole, Jr., *Electron Spin Resonance*, 2nd ed. (Dover Publications, New York, 1996), p. 512 and references therein.
[35] J. Jin, S. Ohkoshi, and K. Hashimoto, Adv. Mater. (Weinheim, Ger.) **16**, 48 (2004).
[36] E. C. Stoner and E. P. Wohlfarth, Philos. Trans. R. Soc. London, Ser. A **240**, 599 (1948).
[37] D. Kechrakos and K. N. Trohidou, Phys. Rev. B **58**, 12 169 (1998).